Available online at www.sciencedirect.com
ScienceDirect
Materials Chemistry and Physics 106 (2007) 109–119
MATERIALS CHEMISTRY AND PHYSICS
www.elsevier.com/locate/matchemphys

Effect of alloying elements on the isothermal solidification during TLP bonding of SS 410 and SS 321 using a BNi-2 interlayer

M.A. Arafin [a,1], M. Medraj [a,*], D.P. Turner [b,2], P. Bocher [c,3]

[a] *Department of Mechanical and Industrial Engineering, Concordia University, Montreal, Canada H3G 1M8*
[b] *Metallurgical Planning, Pratt & Whitney Canada, Longueuil, Que., Canada J4G 1A1*
[c] *Département de Génie Mécanique, École de Technologie Supérieure, Montréal, Canada H3C 1K3*

Received 25 August 2006; received in revised form 16 May 2007; accepted 19 May 2007

Abstract

The random diffusion of solute atoms during transient liquid phase (TLP) bonding of SS 410 and 321 with nickel-based brazing filler alloy BNi-2 have been modeled using Random Walk Modeling technique. Cumulative probability distributions and probability density functions of isothermal solidification times have been calculated for different process conditions and verified with experimental data. The solubility limit of boron has been found to have decreased from 0.3 at.% at higher temperature bonding operations (1358–1394 K) because of substantial iron-rich base metal dissolution when SS 410 was used as base metals; whereas it remained unchanged for SS 321/BNi-2 combination because of high concentrations of nickel and chromium in the base metal. Silicon diffusion model, based on the EDS analysis, also predicted the isothermal solidification times reasonably well.

Keywords: TLP bonding; Isothermal solidification; Modeling; SS 410; SS 321; BNi-2

1. Introduction

SS 410 and 321 are commonly used in aero-engine hot section components, pump and valve shafts, steam generators, expansion joints, super-heaters and re-heaters, etc. due to their high strength, ductility and resistance to creep and to oxidation damages at elevated temperatures. However, due to hardenability, SS 410 is highly susceptible to the heat affected zone (HAZ) cracking during welding [1] and, many intergranular cracks have been observed in the HAZ of the welded SS 321 components due to reheat cracking which is associated to the relaxation of residual stresses that are induced during cooling from welding temperature [2,3].

Typical high temperature brazing with nickel-based fillers evolved as an effective way to join nickel superalloys and stainless steels because it has the capability of producing oxidation and corrosion resistant, high strength joints suitable for elevated temperature applications [4–7]. However, the melting point depressants in the nickel-based fillers form eutectic structures which are extremely hard and contain very brittle intermetallic compounds that are detrimental to the mechanical properties of the brazed joints. There exists a hybrid joining process which can prevent the formation of the abovementioned deleterious phases. It is known as *transient liquid phase* (*TLP*) *bonding*, alternatively termed as *diffusion brazing* [8,9]. The *TLP bonding* process uses a low melting filler alloy to wet the contacting base material and that subsequently solidifies isothermally via a fast diffusing element, e.g. boron. Unlike conventional brazing, the thermal exposure used for the *TLP bonding* cycle is long enough to induce complete isothermal solidification at the bonding temperature and thus, the formation of eutectic phases is avoided during cooling [10].

For a given operating temperature, *TLP bonding* process relies on the time required to complete the isothermal solidification to prevent the formation of the brittle eutectic phases in the resulting brazed joints. Tuah-Poku et al. [11] derived an expression for the holding time for silver/copper/silver sandwich joints based on stationary solid/liquid interface and their predicted

* Corresponding author. Tel.: +1 514 848 2424x3146; fax: +1 514 848 3175.
E-mail addresses: ma_arafi@encs.concordia.ca (M.A. Arafin), mmedraj@encs.concordia.ca (M. Medraj), Daniel.P.Turner@pwc.ca (D.P. Turner), Philippe.Bocher@etsmtl.ca (P. Bocher).
[1] Tel.: +1 514 848 2424x7095; fax: +1 514 848 3175.
[2] Tel.: +1 450 647 3342; fax: +1 450 647 2319.
[3] Tel.: +1 514 396 8645; fax: +1 514 396 8530.

0254-0584/$ – see front matter © 2007 Elsevier B.V. All rights reserved.
doi:10.1016/j.matchemphys.2007.05.049

values were found to be much higher than the experimentally determined values. Lee et al. [12] suggested that diffusion of the solute atoms into the base metal could actually take place during liquid homogenization, which could result in the formation of second phase precipitates and thus the holding time required for complete isothermal solidification would be considerably reduced. Other models based on migrating solid/liquid interface and solute distribution law have been used by several researchers [4,6,13–17] to predict the isothermal solidification completion times and the formation of second phase precipitates in the substrates for pure nickel, nickel-based single crystal superalloys, Inconel 718, 738, 625 and duplex stainless steel base metals with binary Ni–P and Ni–B, or ternary Ni–Cr–B, or multi-component Ni–Cr–B–Fe–Si filler alloys, and reasonable agreement with the experimental values have been reported. However, modeling studies and experimental investigations of isothermal solidification during TLP bonding of SS 410 and 321 with BNi-2 filler alloy, could not be found in the literature.

Although *TLP bonding* is an excellent bonding technique, the time required to complete isothermal solidification is usually long enough to discourage their potential applications in many industries. Therefore, a better understanding of the effect of other process variables, such as bonding temperature and joint gap, on the time required to complete isothermal solidification, is imperative to reduce the time requirement and thus to optimize the process. By a combination of direct experimentation with computational modeling, the optimum joining parameters, such as joint gap, bonding temperature and holding time can be set prior to actual field trials.

Mathematical modeling coupled with experimental data is widely used to determine the kinetic parameters such as diffusion coefficient of solute atoms into the base alloys during *TLP bonding*. However, when coupling experimental data with the mathematical model, the physical and chemical uncertainties associated with the *TLP bonding* experiments needs to be addressed in a way that it best reflects the diffusion characteristics of the solute atoms into the base alloy. Taking only one or two sets of experimental data, often sufficient to solve the governing diffusion equations, will yield one single diffusion coefficient value which is not representative of real life experiments. Several sets of experimentally determined isothermal solidification times, taking the uncertainties involved in the *TLP bonding* experiments into consideration, are required to obtain the true diffusion characteristics of solute atoms. Also, in conventional modeling technique, these one or two sets of experimental isothermal solidification times are usually taken from the eutectic widths versus square root of holding time diagrams where a linear relationship is assumed, i.e. when the eutectic widths are extrapolated to zero value, the corresponding holding time will represent the isothermal solidification time. This is the biggest source of error because of the extreme difficulty in measuring eutectic widths and also the use of extrapolated values instead of real values. However, the errors could not be avoided in previous studies because it is extremely difficult to obtain the exact isothermal solidification time for constant gap joints as the number of samples required is very high and, linear extrapolation to zero eutectic width is employed to approximate the isothermal solidification time for a given joint width. The problem of getting real experimental isothermal solidification times can be eliminated if V-shaped joints are used to determine the maximum TLP bonding clearances. In order to take into consideration the physical and chemical uncertainties associated with *TLP bonding* experiments, several sets of real experimental data need to be used to determine the range of diffusion coefficients and it can be then modeled as a random number based on the statistical distribution profile being observed, such as normal, weibull, uniform or any other distribution. Such modeling approach is known as Random Walk Modeling and is widely used to simulate the diffusion characteristics of solute atoms in diffusion governing processes [18–21]. However, this approach has not been used so far to simulate the diffusion characteristics of solute atoms into the base alloys during *TLP bonding* and, single sets of kinetic parameters for diffusion of solute atoms continue to appear in the literature which is not representative for real life *TLP bonding* experiments.

Hence, the objectives of this work are to calculate the time required to complete isothermal solidification during transient liquid phase bonding of SS 410 and SS 321 stainless steels with BNi-2 filler alloy using mathematical models based on migrating solid/liquid interface and solute distribution law taking the random diffusion of solute atoms into considerations, and to verify the predicted isothermal solidification times with experimental investigations.

Diffusion models for *TLP bonding* with nickel-based filler alloys containing boron as the major melting point depressant rely on the solubility limit of boron in pure nickel as a reference to form solid solution. This assumption is reasonable when pure nickel or nickel-based superalloys are used as base metals. However, when stainless steels are used as base metals, such as SS 410 and 321, significant amount of iron comes into the melt due to the dissolution of base metal. Therefore, such assumption has to be verified experimentally. It is, therefore, also an objective of this study to verify this assumption when martensitic stainless steel, SS 410, with almost negligible amount of nickel in its composition, and austenitic stainless steel, SS 321, with significant amount of nickel and chromium in its composition, are used as base alloys. Also, the use of silicon, which also acts as a melting point depressant, as a reference element to form solid solution will be verified.

2. Experimental investigations

2.1. Procedures

Wrought SS 410 and 321 alloys, widely used in aero-engine hot section components, were chosen for the current study. Wedge-shaped joint gap specimens with identical base alloys, shown in Fig. 1, were utilized to form an edge groove where the BNi-2 filler paste was placed. The nominal compositions of the base and filler alloys are given in Table 1. The specimen was fixed by tack welds to form a variable joint gap (0–250 μm).

The samples were nicro-blasted, acid cleaned and then subsequently TLP bonded at a vacuum pressure of 1.33 mPa (10^{-5} Torr) according to the matrix shown in Table 2. The bonded samples were prepared metallographically and studied under the optical and scanning electron microscope (SEM) equipped with electron dispersive spectrometry (EDS).

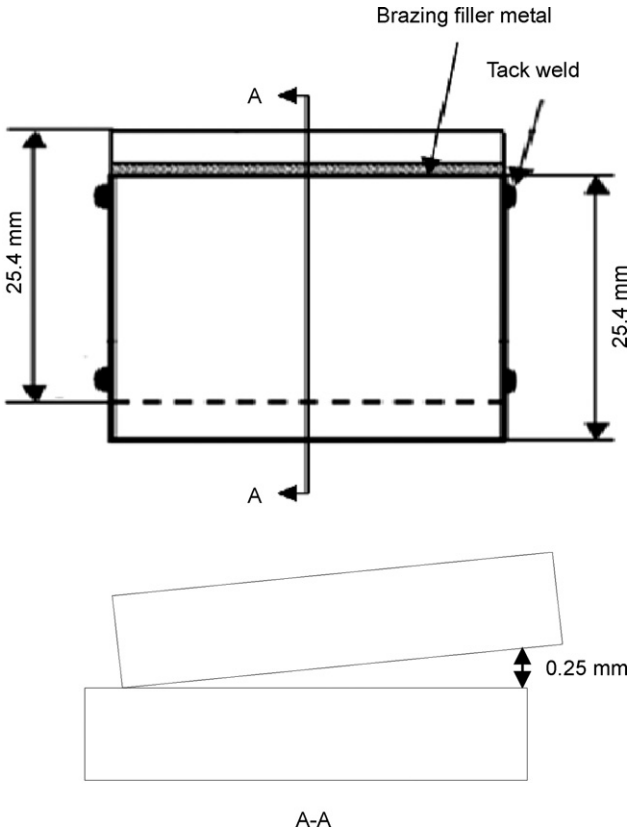

Fig. 1. The wedge-shape joint gap specimen.

2.2. Microstructures of the joints

SEM micrographs of the SS 410/BNi-2 joint are shown in Figs. 2 and 3. Intermetallic phases were formed along the centerline of the joint as the samples were cooled before the isothermal solidification finished. EDS analyses of Fig. 3(a) suggest that the phase marked *X1* is the pro-eutectic γ-*nickel* solid solution and the phases marked with *X2* and *X3* are *Cr*- and *Ni*-rich borides. A line scan through the centerline eutectics of SS 410/BNi-2 joint, shown in Fig. 4, reconfirmed the findings. From the *Ni–Si* phase diagram [22], it is evident that *Ni* dissolves an average of 15 mol% Si over the bonding temperature range (1325–1394 K), and thus it is expected to have little or almost no silicides. However, EDS compositional analyses in Figs. 2–4 revealed a significant amount of silicon in the center of the joint that might form nickel silicides. This can be understood from the following solidification phenomenon [5]: during holding at the bonding temperature, γ-*nickel* first solidified isothermally from the faying surfaces into the melt. Upon cooling the primary γ-*nickel* solidified as nodular dendrites which enriched the remaining melt with boron, silicon and chromium. As cooling proceeded, binary eutectic of γ-*nickel* and *nickel boride* occurred, further enriching the melt of *chromium*. Subsequently, binary eutectic of γ-*nickel* and *chromium boride* solidified. The melt, which was further enriched in silicon, was then transformed into the ternary eutectic of γ-*nickel, nickel boride* and *nickel silicides*. Similar solidification phenomena are expected for the SS 410 and 321 with BNi-2 filler alloy when the holding times are not long enough to complete isothermal solidification.

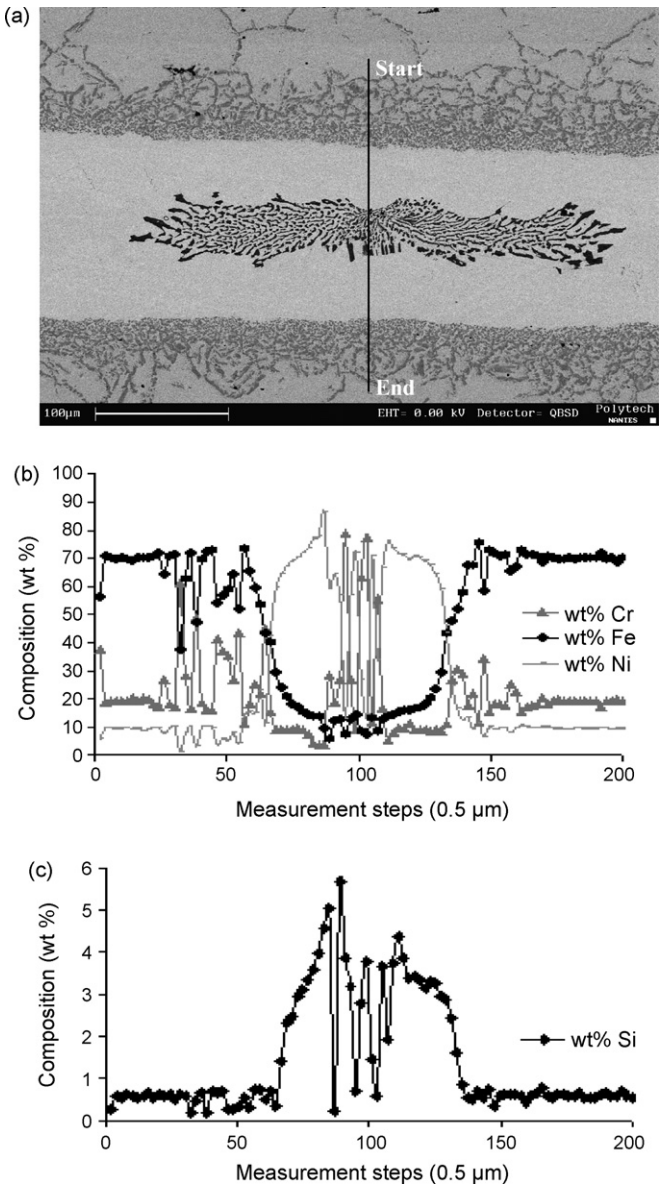

Fig. 2. (a) SEM micrograph of SS 410/BNi-2 joint TLP bonded at 1394 K for 50 min showing centerline eutectics, (b) and (c) EDS analyses.

EDS analyses of Figs. 2–4 also revealed that iron concentration in the joint centerline had reached to 14 wt% and 8 wt%, respectively, for SS 410/BNi-2 joints brazed at 1394 K and 1325 K for 50 min. The initial iron concentration in the BNi-2 filler alloy is 3 wt%, therefore, it is obvious that significant amount of iron has dissolved into the melt due to the dissolution of base metal. The amount of iron increased with increasing bonding temperature because dissolution increases with increasing bonding temperature. Extensive intergran-

Table 1
Nominal compositions of SS 410, SS 321 and BNi-2

Alloy	Nominal composition (wt%)	Solidus (°C)	Liquidus (°C)
SS 410	Fe, <0.15%C, 11.5–13.5%Cr, >0.75%Ni, <1.0%Si, <0.04%P, <0.03%S	1480	1530
SS 321	Fe, <0.08%C, 17–19%Cr, 9.0–12.0%Ni, <0.75%Si, <0.045%P, <0.03%S, <0.7%Ti [5(N + C) min], <0.1%N, <2.0%Mn	1371	1399
BNi-2	Ni–7Cr–3.2B–4.5Si–3Fe–0.06C_{max}	971	999

Table 2
TLP bonding tests matrix

Temperature (K)	Holding time (min)						
1325	10			50	60	70	
1358			30	50		70	90
1394	10	20	30	50			90

ular and transgranular precipitates were also observed at the interface between the base metal and the brazement, as shown in Figs. 2–4. EDS analyses suggest that they are mainly chromium- and iron-rich borides which were also reported by other researchers who worked with BNi-2 filler with different stainless steels such as SS 403, SS 304 and duplex stainless steels UN S31803, etc.

2.3. Maximum TLP bonding clearances

In the wedge gap joint, a distinction is made between areas free of brittle phase and brittle phase containing seam sections. The beginning of brittle phase stabilization marks the maximum *TLP bonding* clearance for the combination of base metals and filler alloy boned at a particular temperature and holding time. Fig. 5 shows the maximum *TLP bonding* clearances for the SS 410/BNi-2 and SS 321/BNi-2 combinations, respectively, brazed at 1325 K, 1358 K and 1394 K with different holding times ranged from 10 min to 90 min. Conversely, if a specified maximum *TLP bonding* clearance is taken, the corresponding holding time will represent the isothermal solidification time for that joint clearance. Significant reduction of holding time has been observed with increasing bonding temperature and/or with decreasing joint gap.

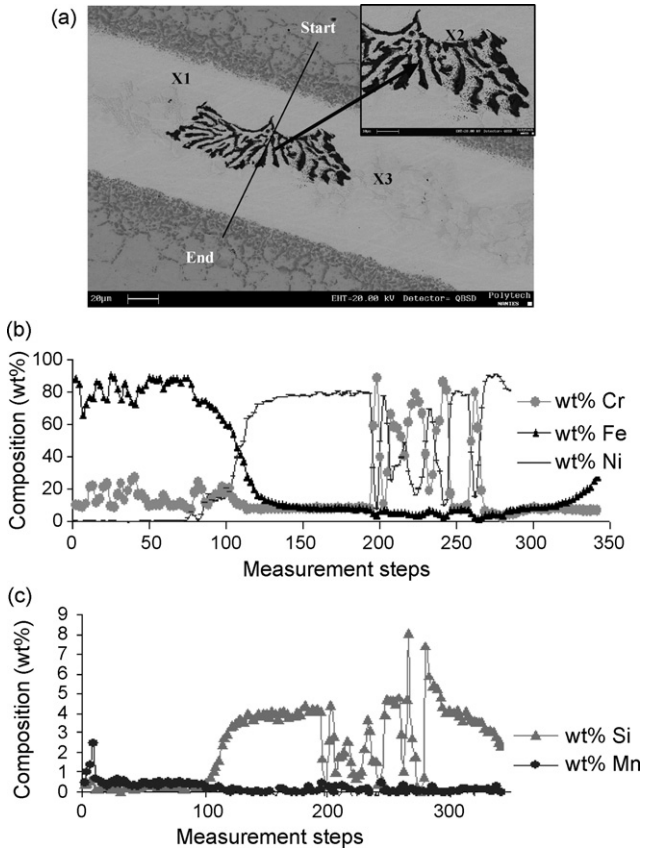

Fig. 3. (a) SEM micrograph of SS 410/BNi-2 joint TLP bonded at 1325 K for 50 min showing centerline eutectics, (b) and (c) EDS analyses.

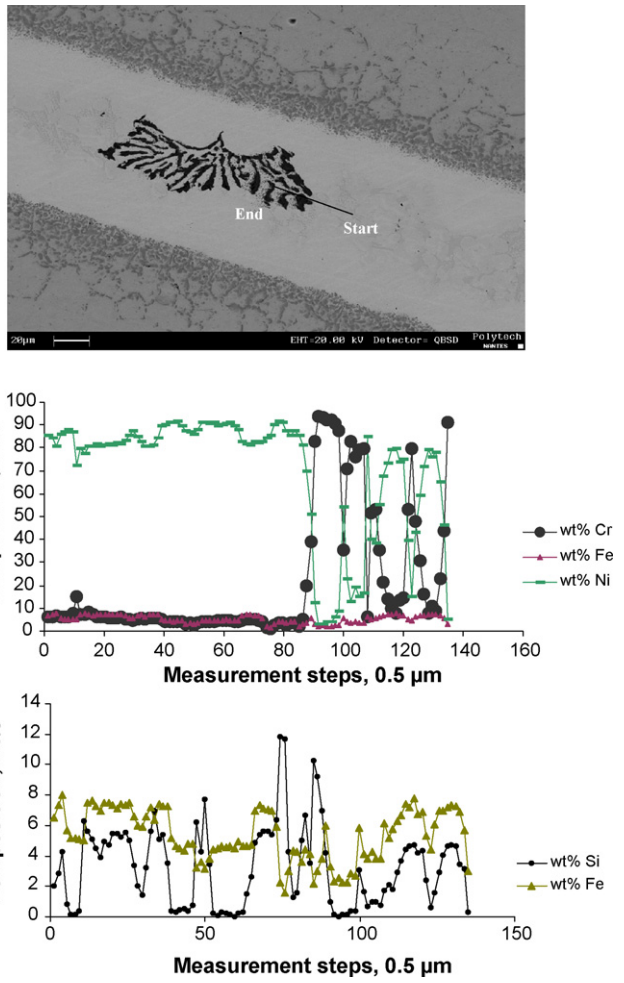

Fig. 4. Line scans through the centerline eutectics of an SS 410/BNi-2 joint TLP bonded at 1325 K for 50 min.

3. Random Walk Modeling of isothermal solidification time

3.1. Migrating solid/liquid interface

According to this modeling approach, the parameter for the moving boundary, γ, can be obtained from the following equation [6,23]:

$$\frac{C_{\alpha L} - C_M}{C_{L\alpha} - C_{\alpha L}} = \gamma\sqrt{\pi}\exp\gamma^2(1 + \mathrm{erf}(\gamma)) \quad (1)$$

where $C_{\alpha L}$ and $C_{\alpha L}$ are the solute concentrations of the solid and liquid phase at the interface, respectively. The completion time for isothermal solidification during *TLP bonding* can then be calculated using the following relation:

$$t_f = \frac{(2h)^2}{16\gamma^2 D} \quad (2)$$

where $2h$ is the maximum width of the molten zone, D is the diffusion coefficient of solute atoms into the base metal and t_f is the time required to complete isothermal solidification.

The *migrating solid/liquid interface model* takes into consideration the moving solid/liquid interface. Moreover, it is

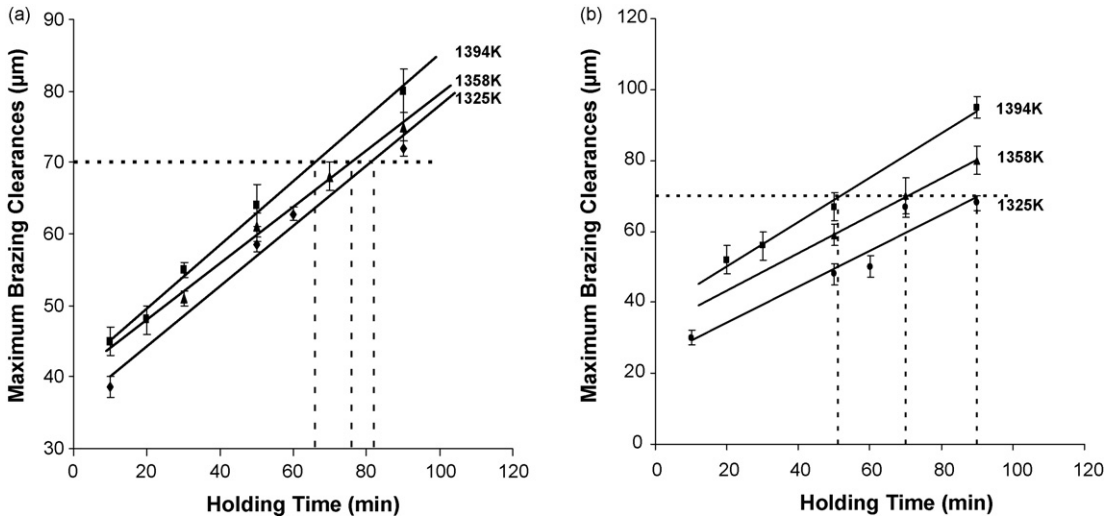

Fig. 5. Effect of holding time on the maximum TLP bonding clearances for (a) SS 410/BNi-2 and (b) SS 321/BNi-2.

coupled with experimental isothermal solidification times to obtain the diffusion coefficients of solute atoms into the base alloys being used. However, as mentioned earlier, there are several physical and chemical uncertainties associated with the experimental investigations which directly affect the kinetics of the diffusion process, and no single value of diffusion coefficient would be representative for real life *TLP bonding* experiments. Physical uncertainties include, but are not limited to (i) waviness of the faying surface, (ii) uncertainties in temperature, time and length measurements, (iii) variation of joint configurations, (iv) heterogeneous wetting of base alloy by the filler alloy, etc. Chemical uncertainties include, but are not limited to, (i) compositional variations of solute atoms in the filler alloy throughout the joint gap, (ii) heterogeneity in the elemental composition of the base alloys, etc. These uncertainties directly affect the assumption of unidirectional diffusion of solute atoms. Therefore, it is quite obvious that diffusion of solute atoms cannot be modeled assuming an ideal case to predict the time required for complete isothermal solidification; rather, it should be modeled taking the random diffusion of solute atoms into considerations due to the physical and chemical uncertainties associated with transient liquid phase bonding experiments. However, the random numbers should be based on the type of statistical distribution, such as normal distribution, weibull distribution, uniform distribution, etc. being observed for diffusion coefficients, obtained from experimentally determined isothermal solidification times, and by taking the mean and standard deviation into considerations. Therefore, such random numbers are based on logical reasoning.

3.2. Modified model equations

The model equations are thus modified as following:

$$D_{i,j} = \frac{(2h_{i,j})^2}{16\gamma^2 t_{f_{i,j}}} \tag{3}$$

where $i = 1, 2, 3, \ldots, n$, which denotes the number of experimentally determined post bonded maximum joint widths free of eutectic phases and the corresponding holding times. $j = 1325$ K, 1358 K, 1394 K, which denotes the bonding temperature.

Diffusion coefficient at a specified bonding temperature can then be written as

$$D_j = [D_{1,j}, D_{2,j}, D_{3,j} \ldots D_{n,j}] \tag{4}$$

If diffusion of solute atoms is modeled as a random number, based on the statistical distribution profile of D_j being observed, diffusion coefficient for a specified bonding temperature can be written as following:

$$D_{\mathrm{R}(j)} = R_{\mathrm{D}_j} \tag{5}$$

where R_{D_j} is a random number based on the statistical distribution profile of D_j, as described before.

Isothermal solidification time for a specified bonding temperature can then be calculated using the following relation:

$$t_{f_{i,j}}^{1/2} = \frac{1}{4\gamma}\left(\frac{2h_{i,j}}{D_{\mathrm{R}(j)}^{1/2}}\right) \tag{6}$$

3.3. Solute distribution modeling

According to Crank [24], for the unsteady state diffusion of a specie present in 2w thick region, into a semi-infinite substrate, solute distribution in the substrate is represented by

$$C_{(y,t)} = C_{\mathrm{m}} + \frac{1}{2}(C_0 - C_{\mathrm{m}})\left\{\mathrm{erf}\frac{y+w}{\sqrt{4Dt}} - \mathrm{erf}\frac{y-w}{\sqrt{4Dt}}\right\} \tag{7}$$

where C_{m} = initial solute concentration in the base metal; C_0 = initial solute concentration in the interlayer; $C_{(y,t)}$ = solute concentration as a function of distance from the centre of the interlayer (y) and time (t); D = diffusion coefficient of the solute in the substrate.

Holding time can be estimated considering the fact that isothermal solidification is completed when the solute concen-

tration at the centre of the interlayer is reduced to the solidus value C_s. Substituting $C_{(y,t)} = C_s$ at $y = 0$ yields the following equation:

$$C_s - C_m = (C_0 - C_m)\left\{\text{erf}\frac{w}{\sqrt{4Dt_f}}\right\} \quad (8)$$

Although this is a simple modeling approach which does not take into consideration the dissolution of base metal, sometimes it can be very useful to have a reasonable approximation of holding time required to complete isothermal solidification during *TLP bonding*. Several researchers [4,14,17,25] used this approach to predict the isothermal solidification time during TLP bonding and to predict the precipitation of second phases in the substrate and reported reasonable agreement with experimentally determined values. However, they used the linear relationships between the eutectic width and square root of holding time to get the extrapolated isothermal solidification times. This approach suffers from the drawback that the time used in the model equation is not the actual one. Also, the complexity in measuring exact eutectic width poses a big challenge on the assumption of linear relationship between the eutectic width and square root of holding time. Moreover, they used only two sets of data to solve the diffusion equations, which is not representative for real life transient liquid phase bonding experiments that involve numerous physical and chemical uncertainties as mentioned earlier. Therefore, similar approach has been used to modify the *solute distribution model* equations. Since the initial composition of boron in both SS 410 and SS 321 is negligible, $C_m = 0$, Eq. (8) can be modified as following:

$$D_{i,j} = \frac{w_{i,j}^2}{(\text{erf}^{-1}C_s/C_0)^2 \times 4 \times t_{i,j}} \quad (9)$$

where $w_{i,j}$ are the halves of the maximum *TLP bonding* clearances obtained experimentally and $t_{i,j}$ are the corresponding holding times.

The isothermal solidification time can then be predicted using the following equation:

$$t_{i,j} = \frac{w^2}{(2\,\text{erf}^{-1}(C_s/C_0)\sqrt{R_{D_j}})^2} \quad (10)$$

where w is half of the initial joint gap thickness for which the isothermal solidification time is to be calculated.

3.4. Summary of the proposed methodology

TLP bonding experiments using wedge-shaped joints enabled determining maximum *TLP bonding* clearances and, thus, the ranges of diffusion coefficients for different bonding temperatures using migrating solid/liquid interface and solute distribution models. Isothermal solidification times for different process conditions were then predicted using Random Walk Modeling and verified with the experimentally determined values. The flow chart shown in Fig. 6 illustrates the methodology used in the current study.

4. Results and discussions

4.1. Migrating solid/liquid interface model

Boron has very low solubility in nickel. Previous investigation [4] on *TLP bonding* with nickel-based filler alloy have suggested that the presence of small amount of additional alloying elements does not change the $C_{\alpha L}$ and $C_{L\alpha}$ values significantly from those of the *Ni–B* system. Similar approach was also used by other researchers [6,15,25] since the solubility of

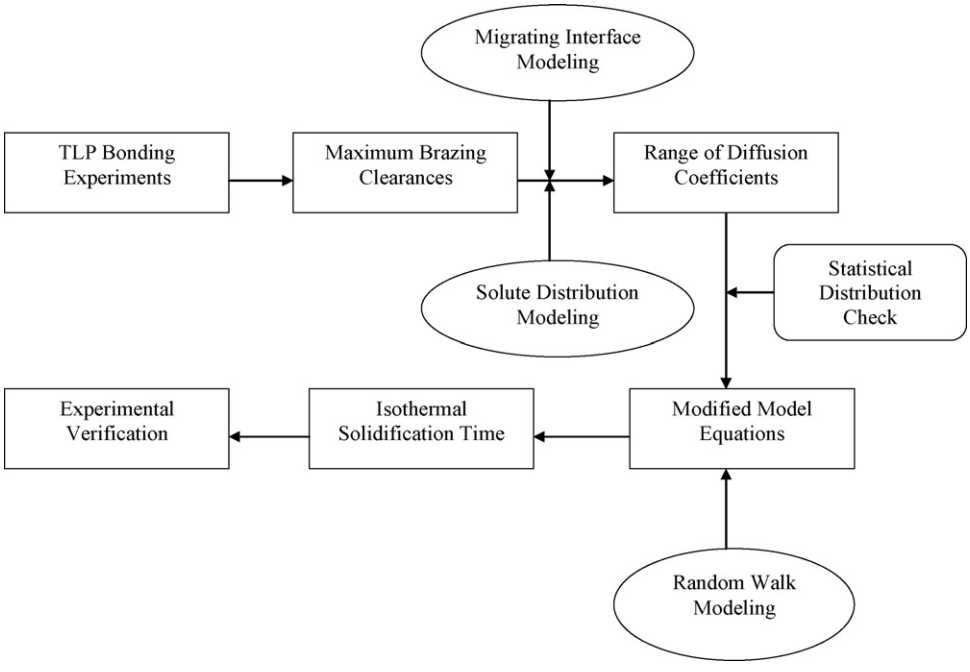

Fig. 6. Flow chart illustrating the methodology of the current study.

Table 3
Range of diffusion coefficients for SS 410/BNi-2 combination

Bonding temperature (K)	Diffusion coefficients ($m^2\ s^{-1}$) $\times 10^{-10}$			
	D_{min}	D_{max}	Mean	S.D.
1325	5.40	13.76	7.93	3.92
1358	7.29	9.26	8.13	0.86
1394	10.59	20.34	13.49	3.92

Table 4
Range of diffusion coefficients for SS 321/BNi-2 combination

Bonding temperature (K)	Diffusion coefficients ($m^2\ s^{-1}$) $\times 10^{-10}$			
	D_{min}	D_{max}	Mean	S.D.
1325	4.81	10.38	6.95	2.63
1358	9.07	10.8	9.83	1.58
1394	10.44	16.0	12.79	2.4

solute atoms in the multi-component melt that are practically encountered during TLP bonding are not available in the literature. Therefore, γ was calculated by taking $C_{\alpha L}$ and $C_{L\alpha}$ as the average solidus and liquidus boron compositions of the *Ni–B* system in the bonding temperature range, 0.3 at.% and 16.6 at.%, respectively.

Numerical simulations were carried out using MATLAB 7.0.1 with modified model equations as given earlier. Range of diffusion coefficients for each of the three bonding temperatures have been obtained using 28 sets of experimentally determined post-brazed maximum clearances free of eutectic phases and the corresponding holding times, and are presented in Tables 3 and 4 for SS 410/BNi-2 and SS 321/BNi-2, respectively. The modified migrating solid/liquid interface model has been, then, applied to predict the isothermal solidification time for an initial joint gap of 70 μm and for three different operating temperatures.

Fig. 7(a) and (b) shows the cumulative probability distribution and probability density plots for holding time required to complete isothermal solidification for SS 410/BNi-2 and SS 321/BNi-2, respectively, for 1358 K bonding temperature and 70 μm joint gap. Isothermal solidification time for the process condition has been predicted as a range where different values have different individual probabilities. Cumulative probability distribution is a very useful tool because it is the measure of the probability that isothermal solidification will take place for less than or equal to a given holding time, e.g. a holding time of 60 min would include the probabilities of isothermal solidification times that are less than or equal to 60 min. Therefore, it is a measure of the confidence level that isothermal solidification would take place if the corresponding length of time is elapsed in the furnace at the bonding temperature. For the assembly that requires a high safety factor, isothermal solidification time should be considered as the one that corresponds to a very high CP value, close to 1, to eliminate any possibility of failure due to the formation of brittle eutectic phases.

The predicted isothermal solidification times for three different bonding temperatures with different confidence levels have been compared with experimentally determined values, for an initial joint gap of 70 μm, for both SS 410/BNi-2 and SS 321/BNi-2, as shown in Fig. 8. It should be noted here that a

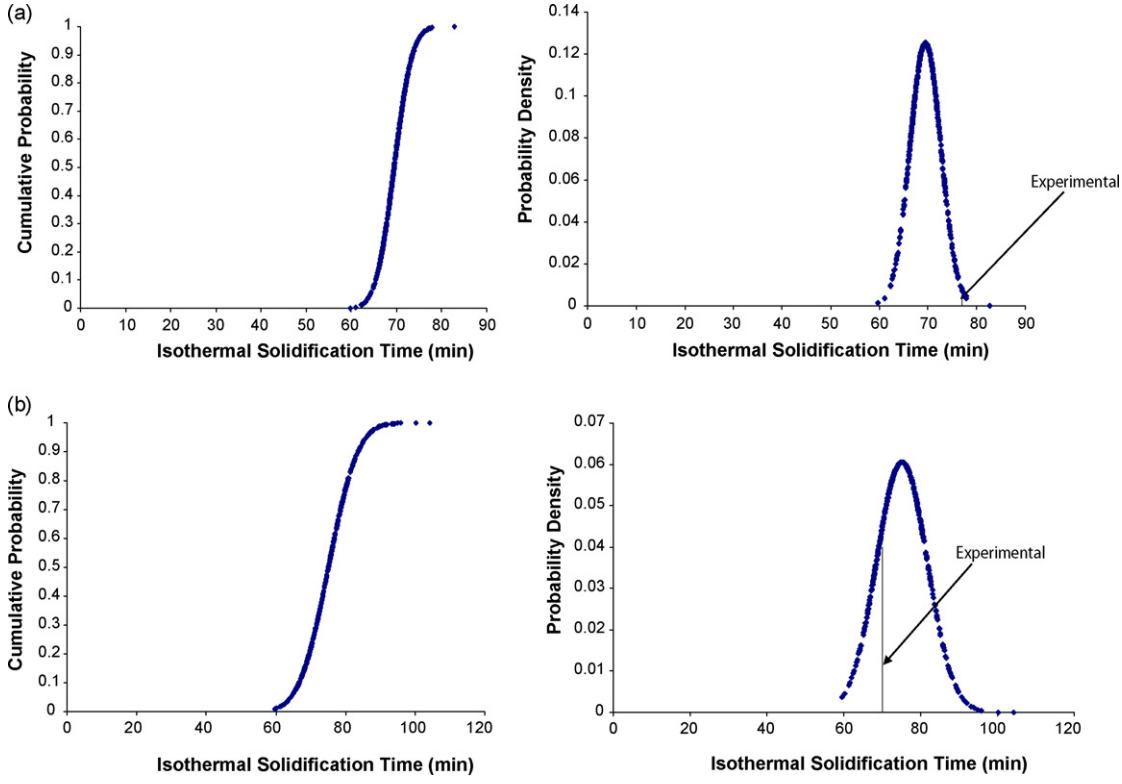

Fig. 7. Cumulative probability plot and probability density plot of isothermal solidification time (modified migrating solid/liquid interface model) for (a) SS 410/BNi-2 and (b) SS 321/BNi-2 for an initial joint gap of 70 μm and 1358 K bonding temperature.

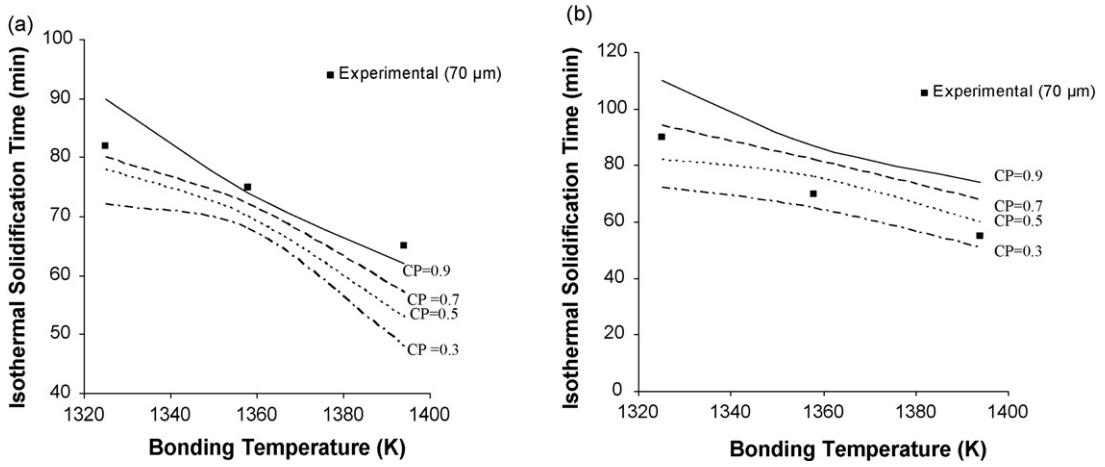

Fig. 8. Comparison of predicted isothermal solidification times with different confidence levels (modified migrating solid/liquid interface model) with experimental data for an initial joint gap of 70 μm for (a) SS 410/BNi-2 and (b) SS 321/BNi-2.

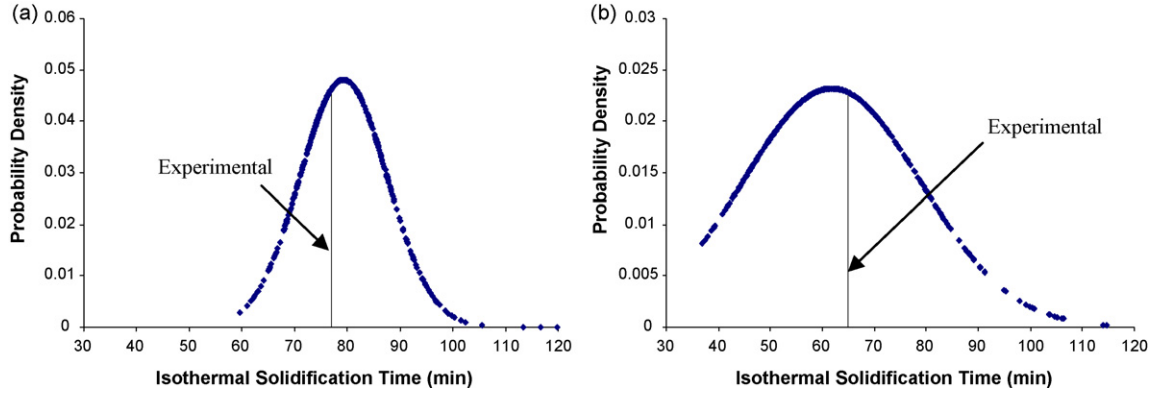

Fig. 9. Verification of decreased boron solubility (0.2 at.%) for SS 410/BNi-2 combinations (modified migrating solid/liquid interface model) with an initial joint gap of 70 μm for (a) 1358 K and (b) 1394 K.

lower confidence level, such as 50% confidence, is not an indication that the probability of occurrence of that event is lower than that of a higher confidence level. In fact, for a perfectly normal distribution, 50% confidence level values have the highest individual probability or, in other words, the maximum likelihoodness. It was interesting to observe that for SS 410/BNi-2, the model underestimated the time requirement at higher temperature bonding operations (1358 K and 1394 K) which suggests that the solubility limit of boron might have decreased. This can be attributed to the following model assumption: the value of $C_{\alpha L}$ and $C_{L\alpha}$ were taken as 0.3 at.% and 16.6 at.%, respectively, which are the average solidus and liquidus boron compositions in the *Ni–B* system at the bonding temperatures [25]. This assumption is reasonable when the base metals are pure nickel or

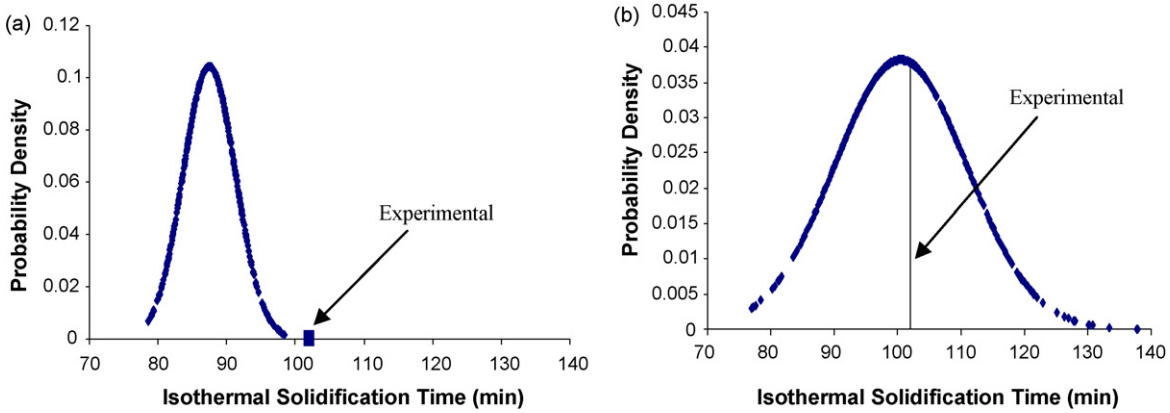

Fig. 10. Verification of decreased boron solubility for SS 410/BNi-2 at 1358 K (modified migrating solid/liquid interface model) with an initial joint gap of 80 μm: (a) 0.3 at.% and (b) 0.2 at.%.

nickel-based superalloys. However, when stainless steels, such as SS 410, are used as base metals, significant amount of iron dissolves due to the dissolution of base metal, especially at higher bonding temperatures; and the assumptions of 0.3 at.% solubility and 16.6 at.% liquidus composition are no longer appropriate. A decrease of solubility limit ($C_{\alpha L}$) or an increase of liquidus composition ($C_{L\alpha}$) will result in an underestimation of the time requirement to complete isothermal solidification. The effect of solubility limit is much higher than that of the liquidus composition, as evident from Eq. (1). The maximum solubility of boron in iron is 0.1 at.% [26] which is one third of that in nickel. Decreased solubility limit of boron in the multi-component melt at higher operating temperature is, thus, justified.

To verify this reasoning, the model was run for a solubility limit of 0.2 at.% for both 1358 K and 1394 K bonding temperatures which showed very good agreement with the experimentally determined values, as shown in Fig. 9. For further verification, the model was also run for 80 μm initial joint gap for both 0.3 at.% and 0.2 at.% boron solubility and compared with the experimentally determined values, e.g. Fig. 10. Again, the model underestimated the isothermal solidification time when 0.3 at.% solubility was used whereas very good agreement was observed for 0.2 at.%. Therefore, it can be inferred that 0.3 at.% solubility can be used to predict the isothermal solidification time requirement at low temperature bonding operation; however, for higher operating temperatures (1358–1394 K) reduced boron solubility should be used for better prediction of isothermal solidification time.

It was interesting to observe that, unlike SS 410/BNi-2 combination, the predicted isothermal solidification times for SS 321/BNi-2 were in good agreement with experimentally determined values in the temperature range being investigated. To verify this observation further, the predicted isothermal solidification times for 80 μm initial joint gap were compared with experimental data which also showed very good agreement, e.g. Fig. 11. This suggests that the assumptions of $C_{\alpha L} = 0.3$ at.% and $C_{L\alpha} = 16.6$ at.% are applicable for SS 321/BNi-2 combination. This can be explained by the fact that unlike SS 410, the amount of nickel and chromium is significant in austenitic stainless steel SS 321, 12 wt% and 19 wt%, respectively, whereas in SS 410, these amounts are 0.75 wt% and 12 wt%, respectively. Although dissolution of base metal brought some iron into the melt, its concentration in the melt is much smaller than that of SS 410-based alloy. Therefore, it can be inferred that the amounts of nickel and chromium in the base metal, as low as 12 wt% and 19 wt%, respectively, can mitigate the effect of iron on the assumption of 0.3 at.% boron solubility as a reference to form solid solution. The solubility limit ($C_s = 0.3$ at.%) will be further verified later with solute distribution model.

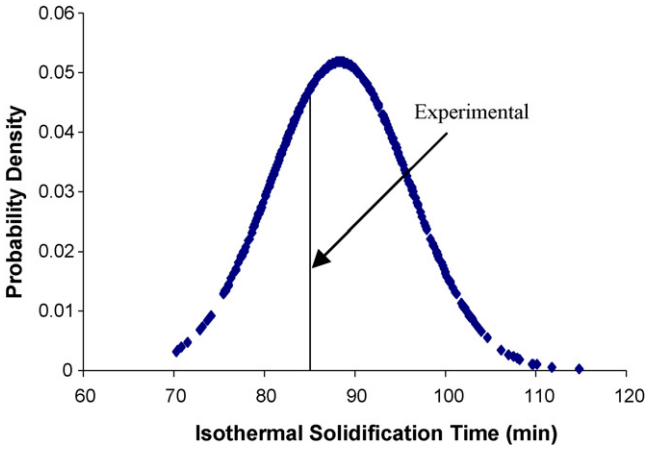

Fig. 11. Verification of 0.3 at.% boron solubility for SS 321/BNi-2 combination (modified migrating solid/liquid interface model) for an initial joint gap of 80 μm at 1358 K.

4.2. Solute distribution modeling approach

Fig. 12 shows the comparison between the predicted isothermal solidification times, for 70 μm initial joint gap at different bonding temperatures, with different confidence levels and experimental data for both SS 410/BNi-2 and SS 321/BNi-2 combinations. The underestimation of isothermal solidification time at 1358 K and 1394 K, for SS 410/BNi-2 combination, which was also observed in migrating solid/liquid interface

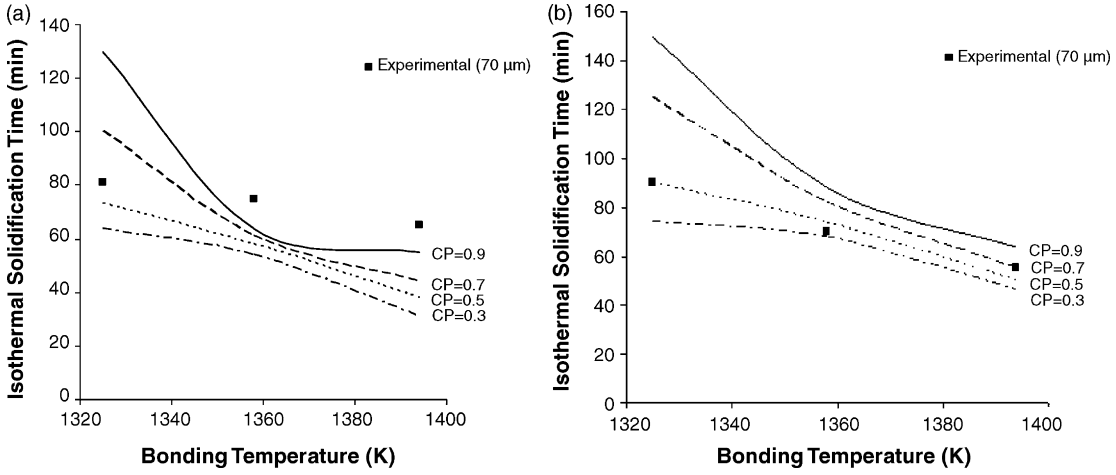

Fig. 12. Comparison of predicted isothermal solidification times with different confidence levels (modified solute distribution model) with experimental data for an initial joint gap of 70 μm for (a) SS 410/BNi-2 and (b) SS 321/BNi-2.

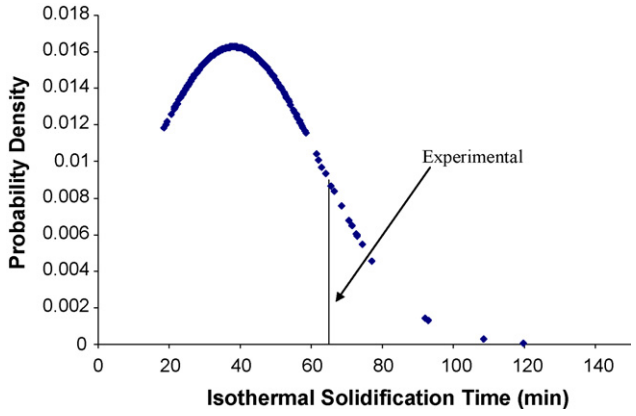

Fig. 13. Verification of 0.2 at.% solubility limit for SS 410/BNi-2 using modified solute distribution model for 1394 K temperature with an initial joint gap of 70 μm.

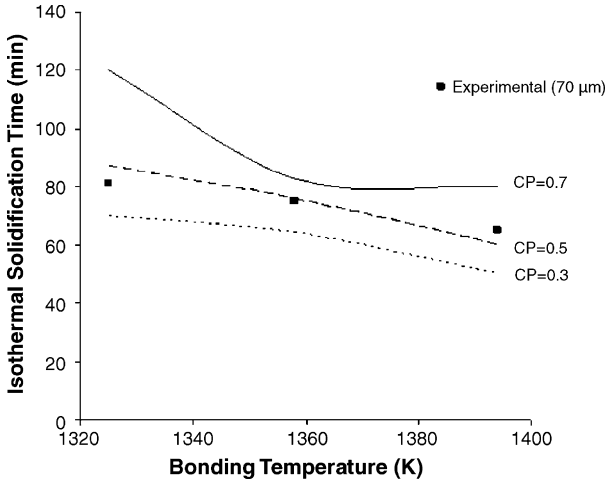

Fig. 14. Comparison of predicted isothermal solidification times with different confidence levels (silicon diffusion model based on solute distribution law) with experimental data for an initial joint gap of 70 μm for SS 410/BNi-2.

model, justifies the reasoning of decreased solubility at higher bonding temperatures.

The simulation results were extended for a solubility limit of 0.2 at.% for 1394 K bonding temperature, as shown in Fig. 13. The predicted values are found to be underestimated compared to that of the migrating solid/liquid interface model as evident from the large distance between the experimentally determined value and the predicted maximum probability density. This can be attributed to the fact that solute distribution model does not take into consideration the dissolution of base metal which is significant at higher temperature bonding operation.

Unlike SS 410/BNi-2 combination, the predicted isothermal solidification times for SS 321/BNi-2 combination were in good agreement in the temperature range being investigated which was also the case with the migrating solid/liquid interface model. This, again, suggests that the assumption of 0.3 at.% solubility is reasonable for SS 321/BNi-2 combination.

4.3. Silicon diffusion model for SS 410/BNi-2

As mentioned earlier, due to the dissolution of base metal, significant amount of iron goes into solution within the joint region during the *TLP bonding* of SS 410/BNi-2 combination. Therefore, taking the boron solubility from the *Ni–B* binary system as a reference to form solid solution is not likely to be appropriate for this system. Like boron, silicon also acts as a melting point depressant which diffuses out from the joint towards the base metal. From the EDS analyses of Fig. 2, the average silicon composition in the isothermally solidified joint area adjacent to the solid/liquid interface was found to be ≈3.16 wt%. Modified solute distribution model equations were then used to predict the times requirement to complete isothermal solidification for an initial joint gap of 70 μm in a similar way as in the case of boron diffusion model using solute distribution law.

Fig. 14 shows a comparison between the predicted isothermal solidification times for 70 μm wide SS 410/BNi-2 joint with the experimental data. Silicon diffusion model does not neglect the effect of any alloying element on the assumption of reference solubility to form γ-*nickel* solid solution and that is why the predicted isothermal solidification times were in better agreement than the other models that rely on the assumption of 0.3 at.% boron solubility.

5. Conclusions

The kinetics of isothermal solidification during *TLP bonding* of SS 410 and 321 with BNi-2 filler has been studied through migrating solid/liquid interface modeling and solute distribution law. However, unlike conventional modeling approaches, the diffusion of solute atoms have been modeled using the Random Walk Modeling technique which can take into account the physical and chemical uncertainties associated with *TLP bonding* experiments. The modified model equations for both modeling approaches have been developed and presented.

Cumulative probability distribution along with probability density plots of isothermal solidification times were calculated for different process conditions and predicted isothermal solidification times with different confidence levels were compared with experimental data. Higher cumulative probability value should be chosen for the components that requires high safety factor.

Both migrating solid/liquid interface model and solute distribution model have underestimated the time requirement to complete isothermal solidification for SS 410/BNi-2 combination at higher temperature bonding operations (1358–1394 K) which suggests that the solubility limit of boron has decreased in this temperature range. In this study, 0.2 at.% solubility was used for the abovementioned temperature range and good agreement was observed with experimental data. The isothermal solidification times predicted by silicon diffusion model were in reasonable agreement with the experimental data because it does not neglect the effect of any alloying element in the melt on the assumption of reference solubility to form γ-*nickel* solid solution.

Unlike SS 410/BNi-2 combination, the predicted isothermal solidification times for the SS 321/BNi-2 combinations, by both

migrating solid/liquid interface and solute distribution models, were in good agreement with the experimentally determined values due to the presence of significant amount of nickel and chromium in the base metal composition.

Acknowledgements

The authors wish to thank Prof. René LeGall at Université Polytechnique de Nantes (France) for helpful discussions and accessibility to EDS equipments and both CRIAQ (Consortium for Research and Innovation in Aerospace in Quebec) and Pratt & Whitney Canada for the financial support to conduct this research.

References

[1] J.A. Penso, Y.M. Lattarulo, A.J. Seijas, J. Torres, D. Howden, C.L. Tsai, ASME Pressure Vessel Pip. Div. Publicat. 395 (1999) 243–253.
[2] M.T. Cabrillat, P. Allegre, E. Pluyette, B. Michel, Trans. SMiRT 16 (2001) 1–8.
[3] M. Chabaud-Reytier, L. Allais, D. Poquillon, C. Caes-Hogrel, M. Mottot, A. Pineau, Mater. High Temp. 18 (2001) 71–80.
[4] O.A. Ojo, N.L. Richards, M.C. Chaturvedi, Sci. Technol. Weld. Join. 9 (2004) 532–540.
[5] S.K. Tung, L.C. Lim, M.O. Lai, Scripta Mater. 34 (1996) 763–769.
[6] A. Sakamoto, C. Fujiwara, T. Hattori, S. Sakai, Weld. J. 68 (1989) 63–71.
[7] O.A. Idowu, N.L. Richards, M.C. Chaturvedi, Mater. Sci. Eng. A 397 (2005) 98–112.
[8] O.A. Ojo, N.L. Richards, M.C. Charturvedi, Sci. Technol. Weld. Join. 9 (2004) 209–220.
[9] C.E. Campbell, W.J. Boettinger, Metall. Trans. A 31 (2000) 2835–2847.
[10] W.F. Gale, Mater. Sci. Forum 426–432 (2003) 1891–1896.
[11] I. Tuah-Poku, M. Dollar, T.B. Massalski, Metall. Trans. A 19 (1988) 675–686.
[12] C.H. Lee, T.H. North, H. Nakagawa, Proceedings of the 71st American Welding Society Convention, Anaheim, CA, 1990, pp. 243–246.
[13] J.E. Ramirez, S. Liu, Weld. J. 71 (1992) 365s–375s.
[14] W.F. Gale, E.R. Wallach, Metall. Trans. A 22 (1991) 2451–2457.
[15] K. Ohsasa, T. Shinmura, T. Narita, J. Phase Equil. 20 (1999) 199–206.
[16] T. Shinmura, K. Ohsasa, T. Narita, Mater. Trans. 42 (2001) 292–297.
[17] M.A. Arafin, M. Medraj, D.P. Turner, P. Bocher, J. Advanced Materials Research vols.15-17 (2007) 882–887.
[18] K.N. Dimou, E.E. Adams, Estuar. Coast Shelf S. 37 (1993) 99–110.
[19] V. Nassehi, S. Passone, Environ. Fluid Mech. 5 (2005) 199–214.
[20] A.W. Visser, Mar. Ecol. Prog. Ser. 158 (1997) 275–281.
[21] C.F. Scott, J. Environ. Eng. 123 (1997) 919–927.
[22] T. Tokunaga, K. Nishio, H. Ohtani, M. Hasebe, Mater. Trans. 44 (2003) 1651–1654.
[23] Y. Zhou, J. Mater. Sci. Lett. 20 (2001) 841–844.
[24] J. Crank, The Mathematics of Diffusion, 2nd ed., Oxford University Press, Oxford, UK, 1975, p. 75.
[25] B. Rhee, S. Roh, D. Kim, Mater. Trans. 44 (2003) 1014–1023.
[26] B. Predel, Phase Equilibria Crystallographic Data and Values of Thermodynamic Properties of Binary Alloys: Group IV: Physical Chemistry, Springler-Verlag/Heidelberg, Berlin/Germany, 1992, p. 15.